Received: 12 April 2018 | Revised: 16 May 2018 | Accepted: 19 May 2018

DOI: 10.1002/mrc.4753

RESEARCH ARTICLE

WILEY

Characterizing gold nanoparticles by NMR spectroscopy

Chengchen Guo | Jeffery L. Yarger

School of Molecular Sciences, Magnetic Resonance Research Center, Arizona State University, Tempe, AZ 85287-1604

Correspondence
Chengchen Guo and Jeffery L. Yarger, School of Molecular Sciences, Magnetic Resonance Research Center, Arizona State University, Tempe, AZ 85287-1604.
Email: cguosci@gmail.com; jyarger@protonmail.com

Funding information
US National Science Foundation, Grant/Award Numbers: NSF DMR BMAT-1809645 and NSF DMR 1264801; US Department of Defence Air Force Office of Scientific Research, Grant/Award Number: FA9550-17-1-0282

Abstract

Gold nanoparticles have attracted considerable attention in recent research because of their wide applications in various fields such as material science, electrical engineering, physical science, and biomedical engineering. Researchers have developed many methods for synthesizing different kinds of gold nanoparticles, where the sizes and surface chemistry of the nanoparticles are considered to be the two key factors. Traditionally, the sizes of nanoparticles are determined by electron microscopy whereas the surface chemistry is characterized by optical spectroscopies such as infrared spectroscopy and Raman spectroscopy. Compared with that, nuclear magnetic resonance (NMR) spectroscopy provides a more advanced and convenient way for size determination and surface chemistry investigations by combining one- and multiple-dimensional NMR spectroscopy and diffusion-order NMR spectroscopy. Here, we show a thorough study that NMR spectroscopy can be applied to characterize small thiol-protected gold nanoparticles, including size determination, surface chemistry investigation, and structural study. The results show that the nanoparticles' sizes determined by NMR agree well with transmission electron microscopy results. Furthermore, the ligand densities of nanoparticles were determined by quantitative NMR spectroscopy, and the structures of ligands capped on the surfaces were studied thoroughly by one- and multiple-dimensional NMR spectroscopy. In this work, we establish a general method for researchers to characterize nanostructures by using NMR spectroscopy.

1 | INTRODUCTION

Noble metal nanomaterials, such as gold/silver nanomaterials, have been studied extensively in recent years because of their wide applications in catalysis, surface-enhanced Raman scattering, biological imaging, drug delivery, and cancer therapy.[1–8] Gold nanoparticles (AuNPs) can be synthesized and functionalized with a variety of ligands through Au—S chemical bonds or electrostatic interaction.[9–14] These ligands control the nucleation and growth of nanoparticles and provide chemical and colloidal stability as well.[15] In order to produce high quality nanoparticles with good size homogeneity, high yield, and satisfied purity, researchers are recently focusing on mechanistic studies of multiple synthetic methods, trying to understand the pathways for controlling the quality of nanoparticles.[16–18] For characterizing AuNPs, many techniques have been developed in the past decades and utilized to investigate the morphologies, structures, optical properties, and surface chemistry of nanoparticles.[15,19] Transmission electron microscopy (TEM) and scanning electron microscopy (SEM) are able to determine the size and to investigate morphology whereas optical spectroscopies such as ultraviolet (UV)–vis spectroscopy, fluorescent spectroscopy, Raman spectroscopy, and infrared spectroscopy are used for understanding the optical

properties and surface chemistry of gold nanomaterials.[15] Recently, mass spectroscopy and single crystal X-ray crystallography have been demonstrated to be excellent tools for characterizing gold nanoclusters. Mass spectroscopy has been used for investigating the ligand density of nanostructures, molecular formula for molecular-like nanoclusters, and charge state of nanoclusters.[20–22] Single crystal X-ray crystallography not only can determine the size of the nanostructures but also the exact stacking patterns of atoms. However, this technique requires sufficient very good quality single crystals to give well-defined diffractions, which limits the technique to be utilized extensively. Until recently, only the structures of $Au_{23}(SC_6H_{11})_{16}$,[23] $Au_{25}(PET)_{18}$,[24] $Au_{25}(SEt)_{18}$,[25] $Au_{28}(TBBT)_{20}$,[26] $Au_{36}(SPh\text{-}tBu)_{24}$,[27] $Au_{38}(SR)_{24}$,[28] and Au_{102} (p-MBA)$_{44}$[29] have been successfully determined by X-ray crystallography. Comparing with all these techniques, nuclear magnetic resonance (NMR) spectroscopy has been demonstrated to be a universal and versatile technique for characterization of nanomaterials.[20,30–33] One-dimensional/multidimensional NMR spectroscopy combined with homonuclear/heteronuclear NMR spectroscopy provides considerable methods for characterizing nanostructures including purity, ligand density, and surface chemistry.[34–38] Furthermore, diffusion-ordered NMR spectroscopy (DOSY)[39] is able to determine the size of nanoparticles in solution state.[40–43]

In this paper, we provided a thorough study that NMR spectroscopy could be applied as a universal tool for characterizing different types AuNPs, determining the purity, size, structure of ligand, and even the Au/ligand ratio. Briefly, ^{1}H direct, two-dimensional (2D) correlation spectroscopy (COSY), and 2D heteronuclear single quantum correlation (HSQC) spectroscopy were performed to investigate the ligand structures on the surfaces and to determine the purity and Au/ligand ratio. DOSY was applied to measure the diffusion coefficient of ligands binding to the nanostructures, which is further used to estimate the diameter of the nanoparticles. By combining different kinds of NMR spectroscopy techniques, the purity, size, and surface chemistry of AuNPs can be characterized very efficiently in time and cost.

2 | EXPERIMENTS

2.1 | Chemicals and materials

Gold (III) chloride hydrate ($HAuCl_4 \cdot 3H_2O$, 99.999%), octanethiol ($C_8H_{17}SH$, 98.5%), tetraoctylammonium bromide (TOAB, 98%), sodium borohydride ($NaBH_4$, ≥99%), L-glutathione, reduced (≥99%, Aldrich), toluene (ACS reagent, ≥99.5%), methanol (ACS reagent, ≥99.8%), ethanol (ACS reagent, ≥99.5%), acetonitrile (ACS reagent, ≥99.5%), and isopropyl alcohol (ACS reagent, ≥99.5%) were purchased from Sigma-Aldrich, and all chemicals were used as received. Deuterated chloroform ($CDCl_3$, 99.9%) and deuterated water (D_2O, 99.9%) were purchased from Cambridge Isotope Inc. and was used as received.

2.2 | Synthesis of octanethiol-capped AuNPs ($C_8H_{17}S$-AuNPs)

$C_8H_{17}S$-AuNPs were prepared as follows. Briefly, an aqueous solution of $HAuCl_4 \cdot 3H_2O$ (39.4 mg, 0.10 mmol, 5 ml, 1 equiv) was mixed with a solution of TOAB in toluene (136.7 mg in 5 ml, 0.25 mmol, 2.5 equiv). The two-phase mixture was rapidly stirred until Au^{3+} was all transferred to the organic phase to give a wine-red solution. The [TOA][AuX_4] was produced with a mix of Cl^- and Br^- ions. After removing the aqueous phase, the organic phase was cooled to ~0 °C in the ice bath, followed by adding in $C_8H_{17}SH$ (70 μl, 0.40 mmol, 4 equiv). The solution was then slowly stirred for about 2 hr until the solution became clear. A freshly prepared ice-cold aqueous solution of $NaBH_4$ (2 ml, 0.5 mol/L, 1.0 mmol) was added to the reaction mixture with vigorous stirring. After 3 hr of reaction, the ice bath was removed, and the solution was continuously stirred for over 24 hr. The long aging time will influence the purity and yield of Au clusters markedly. After reaction was done, the organic phase was separated out and dried under vacuum. The dry product was then washed with methanol and ethanol three times, respectively, to remove excess thiols and byproducts. The pure $C_8H_{17}S$-AuNPs were extracted with pure chloroform.

2.3 | Synthesis of glutathione-capped AuNPs (GS-AuNPs)

In a typical synthesis, an aqueous solution of 20 mM $HAuCl_4$ (5 ml) and 50 mM glutathione (GSH, 3 ml). The mixture was then vigorously stirred for 2 min until the yellowish solution turned cloudy. After being stirred, 1.0 ml 1.0 M NaOH was added to the solution to adjust the pH to basic condition, which made the color of the solution turn clear yellow. Thereafter, diluted 40 μl of $NaBH_4$ (35 mM) was slowly added dropwise. The solution slowly turned orange in the first several minutes. After stirring for 30 min, 1.0 ml 1.0 M HCl was introduced to the solution to readjust the pH to acidic condition, which quench the BH_4^- activity and stirred slowly (150 rpm) for overnight at room temperature. The GS-AuNPs were purified from the raw product using water-IPA mixtures. Typically, the raw solution was mixed with 12 ml IPA to induce the precipitation of the byproducts. After that, the supernatant fluid was separated by centrifugation, and

2.0 ml of IPA was added to the supernatant to induce additional precipitation. Then, the GS-AuNPs were further extract from the precipitation using ultrapure water.

2.4 | TEM and UV–vis spectroscopy characterizations

TEM images were taken using CM200-FEG high-resolution TEM operating at a bias voltage of 200 kV. The TEM samples were prepared by evaporating diluted nanoparticle solution on the carbon-coated copper grid. The images were analyzed using ImageJ software. UV–vis and luminescence spectra were collected using Vernier UV–vis spectrometer, and 1.0 ml of diluted solution was used in each experiment.

2.5 | Thermal gravimetric analysis (TGA)

TGA experiments were performed on a TA2910 (TA Instrument Inc.) under N_2 flow (40 ml/min for furnace and 30 ml/min for balance). The heating rate was 5 °C/min, and 1–2 mg of the sample was used. Before experiment, the sample was kept under a N_2 flow for 10 min to remove most of the physisorbed water and obtain a stable baseline.

2.6 | NMR spectroscopy

The AuNPs and pure thiols were dissolved in deuterated solvents, resulting in 600 μl solution for each sample. All NMR tubes were flame sealed to prevent solvent evaporation and concentration change during the characterization. NMR analysis was conducted on a Varian 500 spectrometer equipped with $^{1}H/^{13}C/^{15}N$ 5 mm XYZ PFG triple-resonance probe using standard VNMRJ software. All experiments were performed with ^{1}H 90° pulse of 7.30 μs and ^{13}C 90° pulse of 31.0 μs at 298.15 K. One-dimensional (1D) ^{1}H spectra were collected with a sweep width of 8012.8, an acquisition time of 2.045 s, a recycle delay of 2.5 s, and 128 scans and 8 scans for gold nanoparticleAuNPs and pure thiols, respectively. In the quantitative NMR experiment, 64 scans and a recycle delay of 60 s were applied, and the measurement was repeated three times. ^{1}H-^{1}H gradient COSY (gCOSY) were performed with a sweep width of 8012.8 Hz, an acquisition time of 150 ms, 128 points in the indirect dimension, and 128 scans per increment, a recycle delay of 1 s. ^{1}H-^{13}C gradient HSQC (gHSQC) spectroscopy was performed with a sweep width of 8012.8 Hz, an acquisition time of 150 ms, 128 points in the indirect dimension, and 512 scans per increment, a recycle delay of 1 s. DOSY measurements were performed with DOSY bipolar pulse pair stimulated echo pulse sequence. A pulsed gradient duration δ of 2.0 ms incremented from 2.9 to 64.8 g/cm in 32 steps and a pulsed gradient separation Δ of 50 ms were used in the measurements. The spectra were collected with a sweep width of 8012.8 Hz, an acquisition time of 2.045 s, 32 scans, and a recycle delay of 10 s. The reported spectra and diffusion coefficients were obtained using the DOSY toolbox in VNMRJ software. A viscosity (η) value of 0.537 mPa and a self-diffusion coefficient value of 2.23×10^{-9} m^2/s were used for chloroform, and a viscosity (η) value of 0.890 mPa and a self-diffusion coefficient value of 2.300×10^{-9} m^2/s were used for water in gradient field calibration and diffusion coefficient calculations for AuNPs samples at 298.15 K.[44]

3 | RESULTS AND DISCUSSION

3.1 | Synthesis of AuNPs

In this work, two types of thiol-capped AuNPs, $C_8H_{17}S$-AuNPs and GS-AuNPs were prepared. However, their physical and chemical properties are significantly different, $C_8H_{17}S$-AuNPs are organic solvent favorable AuNPs whereas GS-AuNPs are water-soluble and biocompatible AuNPs because glutathione is a tri-peptide (Gly-Cys-Glu).[13,14,37,45] These two types of AuNPs were prepared in this work to better demonstrate the general concept that NMR spectroscopy can be applied to characterize AuNPs regardless of their physical and chemical properties. More than that, GS-AuNPs have great potential in biomedical imaging and drug delivery research due to its biocompatibility and unique luminescent properties.[46] However, few NMR investigations have been carried out on this material. In this work, we show some NMR studies on the luminescent GS-AuNPs.

The as-prepared nanoparticles were characterized with UV–vis/luminescent spectroscopy, TEM, and ^{1}H NMR spectroscopy to verify the success of the synthesis and the purity of the materials (Figures 1–3). From the UV–vis absorption spectra (Figure 1), $C_8H_{17}S$-AuNPs showed step-like multiple bands, indicating it is semiconducting and no surface plasmon resonance band can be observed in optical spectra.[42] For GS-AuNPs, two absorption peaks were observed (450 and 515 nm), which is in good agreement with the characteristic values for luminescent gold nanoclusters reported in previous literatures.[13,14] Furthermore, the GS-AuNPs show red-emitting under UV light of 365 nm, and the luminescent spectrum was collected in this work. The emission wavelength was determined to be a broad band with a peak value of 700 nm. TEM was carried out to determine the size and to investigate the morphologies of the nanoparticles as well. Both kinds of nanoparticles have

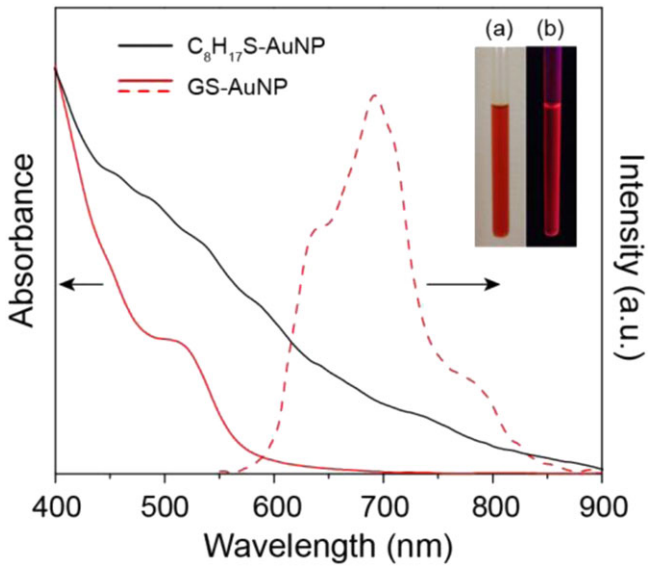

FIGURE 1 Ultraviolet–vis spectra of purified $C_8H_{17}S$-AuNPs and GS-AuNPs (solid lines). Luminescence spectrum of GS-AuNPs (red dashed) with an excitation wavelength of 500 nm. Inset shows the pictures of GS-AuNPs under (a) room light and (b) ultraviolet light (365 nm). AuNPs: gold nanoparticles; GS-AuNPs: glutathione-capped gold nanoparticles

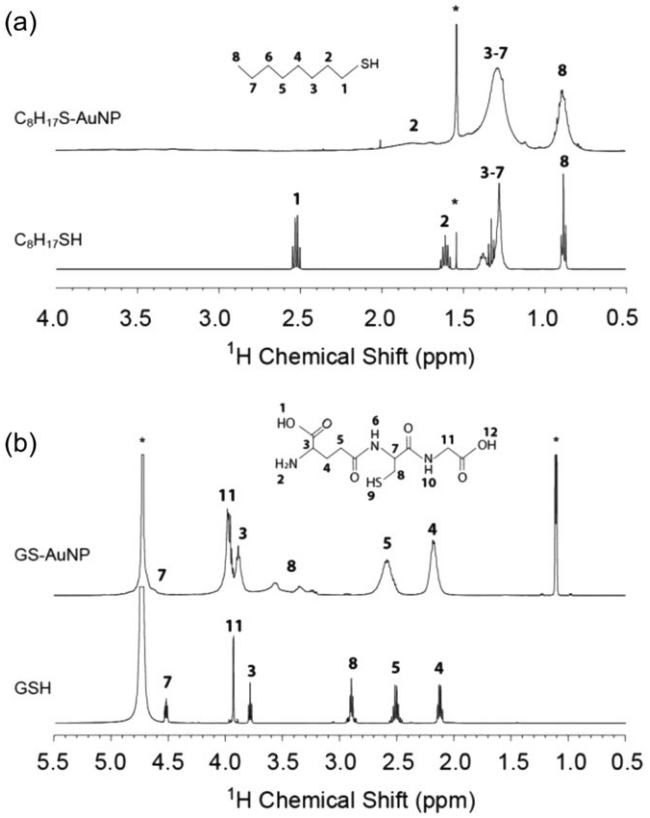

FIGURE 3 ^1H nuclear magnetic resonance spectra of (a) $C_8H_{17}SH$ and $C_8H_{17}S$-AuNP and (b) GSH and GS-AuNPs. * notes the water (1.56 ppm) and isopropyl alcohol (1.1 ppm). AuNPs: gold nanoparticles; GS-AuNPs: glutathione-capped gold nanoparticles; GSH: glutathione

a well-defined spherical shape with diameters of 2.50 ± 0.49 and 1.76 ± 0.47 nm for $C_8H_{17}S$-AuNPs and GS-AuNPs, respectively (Figure 2). The diameters of nanoparticles were determined by analyzing 100 particles for each sample in corresponding TEM profiles. One-dimensional ^1H NMR spectroscopy was applied to check the purity of the prepared nanoparticles and to vfurther obtain some chemical shift information of the ligands binding to the AuNPs (Figure 3). The results indicate that ^1H resonances of thiols binding to the AuNPs surfaces were significantly broadened or shifted or even completely disappeared for both types of AuNPs. For $C_8H_{17}S$-AuNPs, the ^1H resonances of the protons attached to C1 completely disappeared, and the ^1H resonances of the protons attached to C2 was shifted and seriously broadened. For other protons, they showed little chemical shift changes but significant broadening comparing with the pure thiol. The chemical shift change

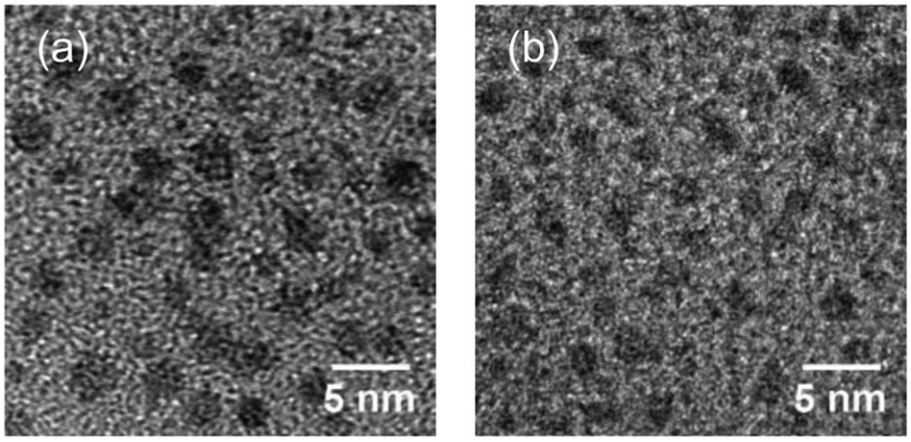

FIGURE 2 Transmission electron microscopy images of (a) $C_8H_{17}S$-AuNPs and (b) GS-AuNPs, respectively. AuNPs: gold nanoparticles; GS-AuNPs: glutathione-capped gold nanoparticles

is due to the structure change of capping groups and proximity to the nanoparticles surfaces, in which $C_8H_{17}SH$ forms Au—S with interfacial gold atoms by eliminating one proton. This affects protons attached to C1 and C2 primarily. The NMR resonance broadening is primarily due to the distribution of the chemical environment (such as $C_8H_{17}S$—Au bonding), and this has been studied and discussed in details in previous research.[35,47] For GS-AuNPs, besides the chemical shift changes for some protons and resonance broadening, the protons attached to C8 showed significant resonance shift, and multiple splitting peaks in a broad chemical shift range, indicating the multiple chemical environment of the GS- ligands at the AuNPs interfaces. The similar results were observed in previous work for Au_{25} $(SG)_{18}$ nanoparticles, and this is attributed to the chirality of the ligands at the interfaces.[37] Briefly, after combining the optical spectroscopy, TEM, and 1D ^{1}H NMR spectroscopy, we conclude that small pure spherical $C_8H_{17}S$-AuNPs and GS-AuNPs were successfully prepared.

3.2 | Surface chemistry and ligand structures at the interfaces

In this work, 2D NMR spectroscopy was performed to investigate the surface chemistry at the interfaces of the AuNPs. Figure 4 shows ^{1}H-^{1}H COSY and ^{1}H-^{13}C HSQC NMR spectra of thiol-capped AuNPs. ^{1}H 1D spectra indicated previously that ^{1}H resonances of ligands were broadened or shifted at the interfaces due to the chemical shift anisotropic effect on AuNPs surfaces. Furthermore, for GS-AuNPs, some ^{1}H resonances show splitting patterns. To understand the splitting patterns and to

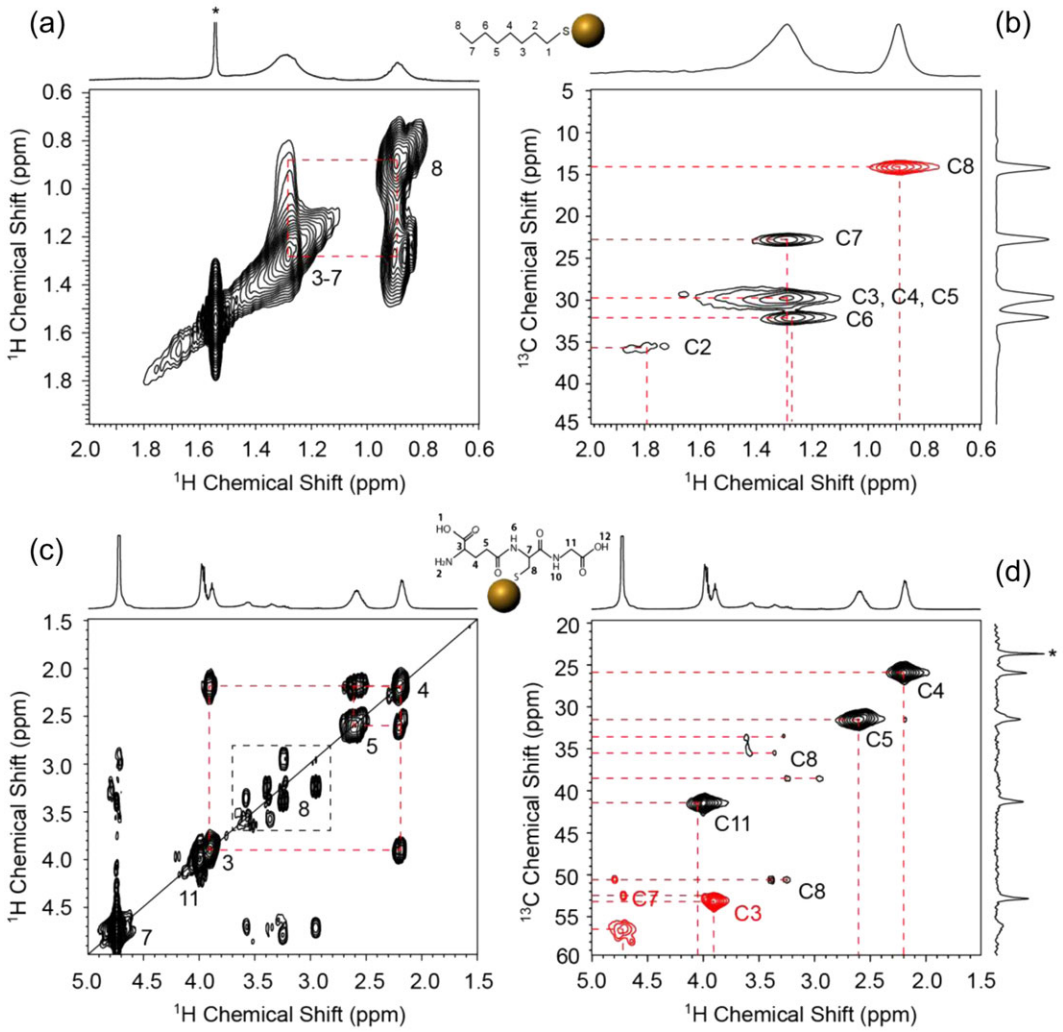

FIGURE 4 ^{1}H-^{1}H correlation spectroscopy nuclear magnetic resonance spectra of (a) $C_8H_{17}S$-AuNP and (c) GS-AuNP, and (b) ^{1}H-^{13}C HSQC nuclear magnetic resonance spectra of $C_8H_{17}S$-AuNP and (d) GS-AuNP, respectively. In HSQC spectra, red indicates CH_2 group whereas black indicates the CH or CH_3 groups. * stands for the water and solvent peak. AuNPs: gold nanoparticles; GS-AuNPs: glutathione-capped gold nanoparticles; HSQC: heteronuclear single quantum correlation

obtain more chemical shift information for other nucleus such as ^{13}C, 2D NMR spectroscopies were utilized in this work and the results are summarized in Table 1. For $C_8H_{17}S$-AuNPs, CH_3 group has a ^1H resonance of 0.9 ppm and a ^{13}C resonance of 14.2 ppm. Most CH_2 groups (C3–C7) have ^1H resonances of around 1.3 ppm and ^{13}C resonances varying from 22.9 to 32.2 ppm (Table 1). ^1H-^1H COSY NMR experiment further showed a strong correlation between CH_3 group and CH_2 groups of the thiol ligand. According to ^1H-^{13}C HSQC NMR spectrum, the C2 group can also be detected, indicating a broad ^1H resonance of 1.80 ppm and ^{13}C resonance of 35.9 ppm. For GS-AuNPs, according to the results, C7 and C8 groups of the ligand have multiple ^1H and ^{13}C resonances, respectively. The multiple ^{13}C resonances for a single group indicate that the surface GS- ligands exhibit multiple chemical environments and may have different types of chemically distinct thiolate-gold binding modes. The ^1H resonance splitting of the 3.3/3.6, 3.4/3.6, 2.9/3.2, and 3.2/3.4 (ppm) pair is caused by the nearby chiral carbon (C8). Due to the size distribution of the synthesized AuNPs and complexity of the molecular structure of gold nanoclusters, the in-depth investigation of the binding modes and chirality-induced splitting was not carried out in this work. However, this idea has been demonstrated and investigated thoroughly on some well-defined AuNPs in previous reported literatures.[20,25,48]

The Au/thiol (Au/SR) ratio of AuNPs can be also obtained with NMR spectroscopy. In this work, we used dimethyl sulfoxide (DMSO) as the internal reference to determine the Au/thiol ratio of purified $C_8H_{17}S$-AuNPs because the ^1H resonances of DMSO (2.6 ppm) and –SR ligand are well separated in the ^1H NMR spectrum. The Au/SR ratio can be determined according to following equations.

$$ratio\left(\frac{Au}{SR}\right) = \frac{n(Au)}{n(SR)} = \frac{Mw(SR)}{Mw(Au)} * \left(\frac{m(AuNP)}{m(SR)} - 1\right), \quad (1)$$

$$m(SR) = \frac{2 * r(CH_3) * Mw(SR) * m(DMSO)}{Mw(DMSO)}, \quad (2)$$

where $n(Au)$ and $n(SR)$ are the moles of gold and thiol ligand, respectively. $Mw(Au)$, $Mw(SR)$, and $Mw(DMSO)$ are the molecular weight of gold, thiol ligand, and DMSO, respectively. $m(AuNP)$, $m(SR)$, and $m(DMSO)$ are the mass of AuNPs, thiol ligand, and DMSO, respectively. $r(CH_3)$ is the ^1H ratio of the methyl group in $C_8H_{17}S$-AuNPs to that in the DMSO.

In this work, 4.04 mg dried purified $C_8H_{17}S$-AuNPs and 2.44 mg DMSO were used for preparing the NMR sample, and 1D ^1H NMR spectrum was collected after sealing the NMR tube. The mass of the ligand on the surface can be calculated by using Equation (2). $r(CH_3)$ is the ^1H ratio of the methyl group in $C_8H_{17}S$-AuNPs to that in the DMSO, and it was estimated to be 0.105 according to the ^1H NMR spectrum (Figure 5). So the Au/SR ratio was calculated to be 2.39. According to the TGA profile of purified $C_8H_{17}S$-AuNPs (Figure S2a), the weight loss was calculated to be 23.2 wt%. Hence, the Au/SR ratio is estimated to be 2.44, which is in good agreement with the quantitative NMR result.

3.3 | Determination of hydrodynamic size using DOSY

The diffusion coefficient of nanoparticles in solution can be well determined by measuring the diffusion coefficient

TABLE 1 Summary of ^1H and ^{13}C resonances of thiols and thiol-capped AuNPs

	$C_8H_{17}SH$		$C_8H_{17}S$-AuNPs		GSH		GS-AuNPs	
Group	^1H (ppm)	^{13}C (ppm)	^1H (ppm)	^{13}C (ppm)	^1H (ppm)	^{13}C (ppm)	^1H (ppm)	^{13}C (ppm)
1	2.53	24.6	—	—	—	—	—	—
2	1.62	34.0	1.80	35.9	—	—	—	—
3	1.38	28.4	1.30[a]	29.9[a]	3.80	55.2	3.91	53.2
4	1.29	29.1	1.30[a]	29.9[a]	2.14	28.5	2.20	25.9
5	1.29	29.1	1.30[a]	29.9[a]	2.53	33.7	2.61	31.5
6	1.27	31.8	1.27	32.2	—	—	—	—
7	1.29	22.5	1.29	23.0	4.54	58.1	4.72	50.5, 52,5, 56.5
8	0.90	14.0	0.89	14.2	2.92	27.9	2.95–3.65	33.5, 35.5, 50.5
11	—	—	—	—	3.96	44.0	3.99	41.3

Note. AuNPs: gold nanoparticles; GS-AuNPs: glutathione-capped gold nanoparticles; GSH: glutathione.

[a]Broad peak with multigroups.

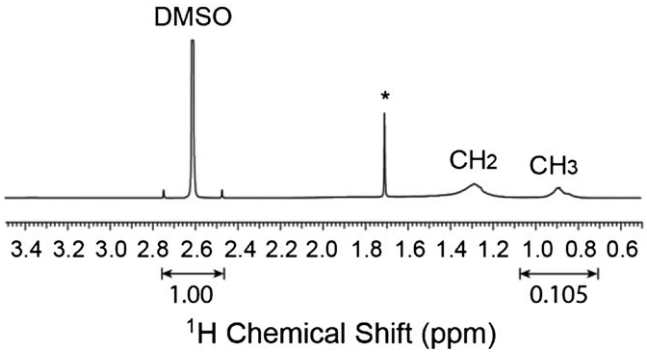

FIGURE 5 ^{1}H nuclear magnetic resonance spectra of purified $C_8H_{17}S$-AuNP with dimethyl sulfoxide at 298 K. * is the water peak. AuNP: gold nanoparticle

of ligands that are covalently bonded to the surfaces of nanoparticle by DOSY. If the diffusion coefficient is determined, the hydrodynamic size of the nanoparticles can be then calculated by using the Stokes–Einstein equation. Diffusion is dependent on the size and shape of individual objects by the well-known Debye–Einstein equation

$$D = \frac{k_b T}{f_T},$$

where k_b is the Boltzmann constant; T is the Temperature in Kelvin; and f_T is the friction factor. For a spherical particle in a homogeneous solution, this equation can be further simplified.

$$D = \frac{k_b T}{6\pi\eta r_H},$$

which is commonly known as the Stokes–Einstein equation. r_H is the hydrodynamic radius; and η is the viscosity of the solvent used. So the hydrodynamic radius of the particles can be calculated on the basis of the following equation:

$$r_H = \frac{k_b T}{6\pi\eta D}.$$

In this work, the diffusion coefficients of $C_8H_{17}S$-AuNPs and GS-AuNPs were determined by DOSY in $CDCl_3$ and D_2O, respectively (Figure 6). The hydrodynamic radii were then calculated according to the Stokes−Einstein equation, giving the average hydrodynamic diameters of 3.28 ± 0.38 and 2.63 ± 0.20 nm for $C_8H_{17}S$-AuNPs and GS-AuNPs, respectively (Table 2). However, TEM results show that the diameters of $C_8H_{17}S$-AuNPs and GS-AuNPs are 2.50 ± 0.49 and

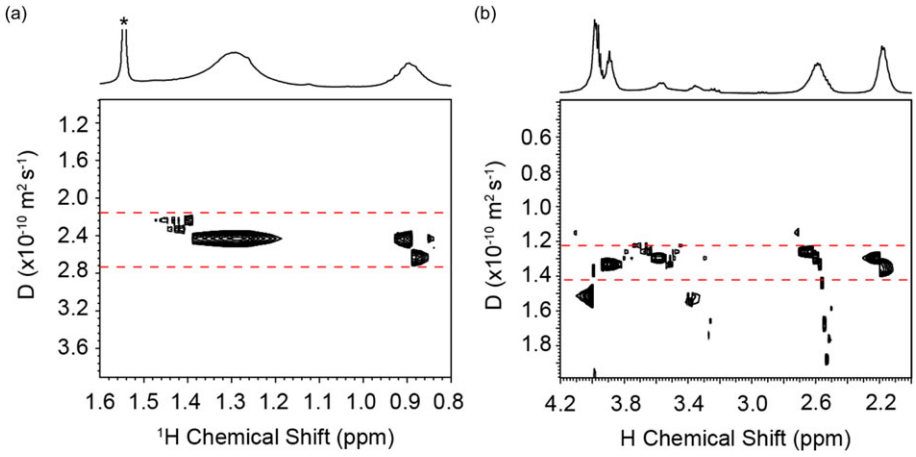

FIGURE 6 Two-dimensional DOSY NMR spectra of (a) $C_8H_{17}S$-AuNPs and (b) GS-AuNPs with $\delta = 2$ ms, $\Delta = 50$ ms at 298 K. AuNPs: gold nanoparticles; DOSY: diffusion-ordered nuclear magnetic resonance spectroscopy; GS-AuNPs: glutathione-capped gold nanoparticles; NMR: nuclear magnetic resonance

TABLE 2 Summary of DOSY experiments on thiol capped gold nanoparticles

Sample	D[a] (m^2/s)	$D_{solvent}$[b] (m^2/s)	r_H (nm)	d_H (nm)	d_{TEM} (nm)
$C_8H_{17}S$-AuNP	$(2.45 \pm 0.28) \times 10^{-10}$	2.17×10^{-9}	1.64 ± 0.19	3.28 ± 0.38	2.50 ± 0.49
$C_8H_{17}SH$	1.40×10^{-9}	2.23×10^{-9}	0.29	0.58	—
GS-AuNP	$(1.32 \pm 0.10) \times 10^{-10}$	1.64×10^{-9}	1.32 ± 0.10	2.63 ± 0.20	1.76 ± 0.47
GSH	3.44×10^{-10}	1.26×10^{-9}	0.39	0.78	—

Note. DOSY: diffusion-ordered nuclear magnetic resonance spectroscopy; TEM: transmission electron microscopy.

1.76 ± 0.47 nm, respectively, which are smaller than the values obtained by DOSY NMR spectroscopy. This is because TEM is mainly focusing on measuring the physical size of the metal core whereas the DOSY NMR spectroscopy measures the effective hydrated diameters of nanoparticles in solution, taking the ligands binding to the surfaces into account. The hydrodynamic diameter of octanethiol and glutathione were measured to be 0.58 and 0.78 nm, respectively. So the estimated hydrodynamic diameter of $C_8H_{17}S$-AuNPs and GS-AuNPs fall in the range of 3.08–3.66 nm for $C_8H_{17}S$-AuNPs and 2.54–3.32 nm for GS-AuNPs, respectively, which agrees well with the hydrodynamic diameter of 3.28 ± 0.38 and 2.63 ± 0.20 nm obtained by the DOSY NMR measurements.

4 | CONCLUSION

In this paper, we showed that NMR spectroscopy is a quite powerful technique for investigating the AuNPs, providing useful and reliable structural and dimensional information. It is shown that HSQC NMR spectroscopy is able to provide chemical shift information that can be further used to study the structure of ligand on the surfaces. Quantitative NMR offers a simple and cost-effective way to determine the Au/SR ratio. Furthermore, hydrodynamic size estimation can be realized by measuring the diffusion coefficient of ligand bounded to the surfaces using DOSY NMR spectroscopy. For recent nanotechnology research, tools for nanomaterials' qualitative and quantitative analysis are of extreme importance, not only for quality control in production but also for applications in various research fields. Based on this work, we showed the great potential of applying NMR spectroscopy in nanomaterials characterizations and expect that NMR spectroscopy including multidimensional NMR spectroscopy and DOSY NMR spectroscopy can be applied to characterize a broad range of nanomaterials including quantum dots, oxide nanoparticles in the future.

ACKNOWLEDGEMENTS

The research was supported by grants from the US National Science Foundation (NSF DMR BMAT-1809645), US National Science Foundation (NSF DMR 1264801) and US Department of Defence Air Force Office of Scientific Research (FA9550-17-1-0282). We thank Dr. Brian Cherry and Dr. Samrat Amin for help with NMR instrumentation, student training, and scientific discussion.

CONFLICTS OF INTEREST

The authors declare no competing financial interest.

ORCID

Chengchen Guo http://orcid.org/0000-0001-9253-3469

REFERENCES

[1] M. Stratakis, H. Garcia, *Chem. Rev.* **2012**, *112*, 4469.

[2] B. Sharma, R. R. Frontiera, A.-I. Henry, E. Ringe, R. P. van Duyne, *Materials Today* **2017**, *15*, 16.

[3] D.-K. Lim, K.-S. Jeon, J.-H. Hwang, H. Kim, S. Kwon, Y. D. Suh, J. M. Nam, *Nat. Nanotechnol.* **2011**, *6*, 452.

[4] P. L. Stiles, J. A. Dieringer, N. C. Shah, R. P. van Duyne, *Annual Rev. Anal. Chem.* **2008**, *1*, 601.

[5] J. K. Yoon, K. Kim, K. S. Shin, *J. Phys. Chem. C* **2009**, *113*, 1769.

[6] R. A. Sperling, P. R. Gil, F. Zhang, M. Zanella, W. J. Parak, *Chem. Soc. Rev.* **2008**, *37*, 1896.

[7] R. Wilson, *Chem. Soc. Rev.* **2008**, *37*, 2028.

[8] V. Marjomaki, T. Lahtinen, M. Martikainen, J. Koivisto, S. Malola, K. Salorinne, M. Pettersson, H. Hakkinen, *Proc. Natl. Acad. Sci.* **2014**, *111*, 1277.

[9] B. V. Enustun, J. Turkevich, *J. Am. Chem. Soc.* **1963**, *85*, 3317.

[10] M. Zhu, E. Lanni, N. Garg, M. E. Bier, R. Jin, *J. Am. Chem. Soc.* **2008**, *130*, 1138.

[11] Z. Wu, J. Suhan, R. Jin, *J. Mater. Chem.* **2009**, *19*, 622.

[12] J. Xie, Y. Zheng, J. Y. Ying, *J. Am. Chem. Soc.* **2009**, *131*, 888.

[13] Y. Yu, Z. Luo, D. M. Chevrier, D. T. Leong, P. Zhang, D.-E. Jiang, J. Xie, *J. Am. Chem. Soc.* **2014**, *136*, 1246.

[14] K. Pyo, V. D. Thanthirige, K. Kwak, P. Pandurangan, G. Ramakrishna, D. Lee, *J. Am. Chem. Soc.* **2015**, *137*, 8244.

[15] M. Grzelczak, J. Pérez-Juste, P. Mulvaney, L. M. Liz-Marzán, *Chem. Soc. Rev.* **2008**, *37*, 1783.

[16] P. J. G. Goulet, R. B. Lennox, *J. Am. Chem. Soc.* **2010**, *132*, 9582.

[17] L. Zhu, C. Zhang, C. Guo, X. Wang, P. Sun, D. Zhou, W. Chen, G. Xue, *J. Phys. Chem. C* **2013**, *117*, 11399.

[18] C. Yu, L. Zhu, R. Zhang, X. Wang, C. Guo, P. Sun, G. Xue, *J. Phys. Chem. C* **2014**, *118*, 10434.

[19] H. Häkkinen, *Nat. Chem.* **2012**, *4*, 443.

[20] Z. Wu, C. Gayathri, R. R. Gil, R. Jin, *J. Am. Chem. Soc.* **2009**, *131*, 6535.

[21] H. Hinterwirth, S. Kappel, T. Waitz, T. Prohaska, W. Lindner, M. Lämmerhofer, *ACS Nano* **2013**, *7*, 1129.

[22] N. K. Chaki, Y. Negishi, H. Tsunoyama, Y. Shichibu, T. Tsukuda, *J. Am. Chem. Soc.* **2008**, *130*, 8608.

[23] A. Das, T. Li, K. Nobusada, C. Zeng, N. L. Rosi, R. Jin, *J. Am. Chem. Soc.* **2013**, *135*, 18264.

[24] M. W. Heaven, A. Dass, P. S. White, K. M. Holt, R. W. Murray, *J. Am. Chem. Soc.* **2008**, *130*, 3754.

[25] T. Dainese, S. Antonello, J. A. Gascón, F. Pan, N. V. Perera, M. Ruzzi, A. Venzo, A. Zoleo, K. Rissanen, F. Maran, *ACS Nano* **2014**, *8*, 3904.

[26] C. Zeng, T. Li, A. Das, N. L. Rosi, R. Jin, *J. Am. Chem. Soc.* **2013**, *135*, 10011.

[27] C. Zeng, H. Qian, T. Li, G. Li, N. L. Rosi, B. Yoon, R. N. Barnett, R. L. Whetten, U. Landman, R. Jin, *Angew. Chem. Int. Ed.* **2012**, *51*, 13114.

[28] H. Qian, W. T. Eckenhoff, Y. Zhu, T. Pintauer, R. Jin, *J. Am. Chem. Soc.* **2010**, *132*, 8280.

[29] P. D. Jadzinsky, G. Calero, C. J. Ackerson, D. A. Bushnell, R. D. Kornberg, *Science* **2007**, *318*, 430.

[30] C. Guo, G. P. Holland, *J. Phys. Chem. C* **2014**, *118*, 25792.

[31] C. Guo, G. P. Holland, *J. Phys. Chem. C* **2015**, *119*, 25663.

[32] C. Guo, G. P. Holland, J. L. Yarger, *MRS Adv.* **2016**, *1*, 2261.

[33] C. Guo, J. S. Jordan, J. L. Yarger, G. P. Holland, *ACS Appl. Mater. Interfaces* **2017**, *9*, 17653.

[34] G. C. Lica, B. S. Zelakiewicz, Y. Y. Tong, *J. Electroanal. Chem.* **2003**, *554-555*, 127.

[35] B. S. Zelakiewicz, A. C. de Dios, *J. Am. Chem. Soc.* **2003**, *125*, 18.

[36] Z. Wu, R. Jin, *ACS Nano* **2009**, *3*, 2036.

[37] H. Qian, M. Zhu, C. Gayathri, R. R. Gil, R. Jin, *ACS Nano* **2011**, *5*, 8935.

[38] L. E. Marbella, J. E. Millstone, *Chem. Mater.* **2015**, *27*, 2721.

[39] K. F. Morris, C. S. Johnson, *J. Am. Chem. Soc.* **1992**, *114*, 3139.

[40] Z. Tang, B. Xu, B. Wu, M. W. Germann, G. Wang, *J. Am. Chem. Soc.* **2010**, *132*, 3367.

[41] G. Canzi, A. A. Mrse, C. P. Kubiak, *J. Phys. Chem. C* **2011**, *115*, 7972.

[42] K. Salorinne, T. Lahtinen, J. Koivisto, E. Kalenius, M. Nissinen, M. Pettersson, H. Häkkinen, *Anal. Chem.* **2013**, *85*, 3489.

[43] K. Salorinne, T. Lahtinen, S. Malola, J. Koivisto, H. Häkkinen, *Nanoscale* **2014**, *6*, 7823.

[44] H. Kato, T. Saito, M. Nabeshima, K. Shimada, S. Kinugasa, *J. Magn. Reson.* **2006**, *180*, 266.

[45] Y. Negishi, K. Nobusada, T. Tsukuda, *J. Am. Chem. Soc.* **2005**, *127*, 5261.

[46] N. Goswami, F. Lin, Y. Liu, D. T. Leong, J. Xie, *Chem. Mater.* **2016**, *28*, 4009.

[47] R. Sharma, G. P. Holland, V. C. Solomon, H. Zimmermann, S. Schiffenhaus, S. A. Amin, D. A. Buttry, J. L. Yarger, *J. Phys. Chem. C* **2009**, *113*, 16387.

[48] O. A. Wong, C. L. Heinecke, A. R. Simone, R. L. Whetten, C. J. Ackerson, *Nanoscale* **2012**, *4*, 4099.

SUPPORTING INFORMATION

Additional supporting information may be found online in the Supporting Information section at the end of the article.

How to cite this article: Guo C, Yarger JL. Characterizing gold nanoparticles by NMR spectroscopy. *Magn Reson Chem*. 2018;56: 1074–1082. https://doi.org/10.1002/mrc.4753